2

DOE/PC/92547--1

DE93 009676

TECHNICAL PROGRESS REPORT

for the First Quarter

(October 1, 1992 to December 31, 1992)

STUDIES OF INCIPIENT OXIDATION OF COAL-PYRITE FOR IMPROVED PYRITE REJECTION

by

R.-H. Yoon and P.E. Richardson
Department of Mining and Minerals Engineering
Virginia Polytechnic Institute & State University
Blacksburg, Virginia 24061-0258

Grant Number:
DE-FG22-92PC92547

Project Manager:

Richard Read
U.S. Department of Energy
Pittsburgh Energy Technology Center
P.O. Box 10940
Pittsburgh, Pennsylvania 15236

U.S./DOE Patent Clearance is not required prior to the publication of this document.

ABSTRACT

In order to foster the development of advanced coal cleaning technologies, fundamental studies of the initial stages of pyrite oxidation have been initiated. This work is being done on pyrite surfaces that are freshly fractured in an electrolyte solution. This procedure produces surfaces that are initially unoxidized, allowing the subsequent oxidation processes to be studied in detail. It is shown that freshly fractured pyrite electrodes instantaneously (at fracture) assume a rest potential several hundred millivolts more negative than the usual open-circuit potential. A finite, anodic photocurrent, is also observed on the fractured electrodes. Following cleavage, the rest potential increases, indicating an oxidation reaction occurring on the electrodes. The photocurrent is relatively insensitive to this oxidation process, and to moderate anodic and cathodic polarization. However, strong cathodic polarization to about -0.76 V (SHE) at pH 9.2 causes the photocurrent to decrease to zero. No reversal in the sign of the photocurrent is observed and it is believed that the flat band potential occurs near -0.76 V, i.e., where the photocurrent goes to zero. Voltammetry indicates that pyrite also undergoes cathodic decomposition at -0.76 V. This establishes that pyrite must be cathodically decomposed to reach the flat band potential.

TABLE OF CONTENTS

LIST OF FIGURES

INTRODUCTION

The superficial oxidation of pyrite creates a problem in removing pyrite from coal using flotation or oil agglomeration processes. This problem is related to the hydrophobic nature of the oxidation products. Flotation induced by superficial oxidation of sulfides is referred to as *self-induced* or *collectorless* flotation. Self-induced flotation has only recently been recognized as significant in sulfide flotation (1,2), and essentially results from the superficial oxidation of sulfide minerals producing a sulfur-rich surface; the excess sulfur is in the form of elemental sulfur or polysulfides depending on the pH. These sulfur oxidation products are naturally hydrophobic and, therefore, render sulfide minerals hydrophobic. The identification of these products has resolved the long-standing controversy over whether sulfide minerals are naturally hydrophobic. With the exception of the sulfides with layer structures that are held together by London Van der Waal dispersion forces, it is believed that most sulfides, including pyrite, are naturally hydrophilic but become hydrophobic upon superficial oxidation. In the case of coal pyrite, the kinetics of oxidation depends on the origin of pyrite, possibly because of the differences in solid-state properties. In general, coal-pyrite oxidizes faster than ore-pyrite (3), and self-induced flotation is difficult to suppress.

This project is directed at obtaining a better understanding of pyrite oxidation and developing methods of inhibiting pyrite oxidation. CCMP has recently developed (4) a photoelectrochemical technique of studying incipient oxidation of freshly-fractured pyrite. This technique uses chopped illumination to induce transient photovoltages or photocurrents in semiconducting minerals such as pyrite. The photoresponse is used in studying the initial stages of pyrite

oxidization; determining if the source of pyrite (semiconducting property) affects its oxidation; and developing new methods of preventing or controlling pyrite oxidation.

The objective of the research conducted during the first quarter was to build a suitable cell with an optical window, refine the measurement technique of obtaining photocurrents on fractured electrodes, and to begin to quantify the relationship between the photocurrent and the oxidation of pyrite.

EXPERIMENTAL

A conventional three compartment electrochemical cell with the compartments containing the pyrite working electrode, reference electrode, and platinum counter electrode has been designed and built. The cell contains a quartz window for illumination.

The photocurrent is induced by illumination of the sample with white light from a 100 watt tungsten-halogen lamp. The light is chopped at 40 to 90 Hertz using a chopper built in our lab. The photocurrents are amplified by a PAR 273 potentiostat and the root mean square of the in phase component measured with a PAR 5208 phase sensitive detector. The transient response of the electrodes can also be analyzed by displaying them on a Tektronix 7613 oscilloscope.

Initial experiments have been conducted on mineral pyrite samples from Peru. The samples are cut with a slow speed diamond saw to dimensions of approximately $2x4x10mm^3$. An electrical lead is attached to one $2x4mm^2$ face using conducting silver epoxy or indium solder. The electrode is then attached to a 7 mm glass tube with a non-reactive epoxy (Torr seal, Varian Industries). When attaching the electrode to the glass tube, approximately one half of the sample is encapsulated with epoxy, the other half projecting out of the epoxy. After insertion in the

cell, a sharp tap on a glass rod resting on the projecting portion of the sample is sufficient to fracture the electrode. Usually the fracture occurs flush with, or just beneath, the epoxy so that the entire electrode surface exposed to the electrolyte after fracture represents the unoxidized surface.

Figure 1 schematically illustrates the experimental setup.

RESULTS AND DISCUSSION

Task 1 - Quantification of the photoresponse of *in situ* fractured pyrite as a direct, *in situ* measurement of the semiconducting properties of pyrite.

The open-circuit potential of pyrite at the instant of, and following, fracture at pH 9.2 is shown in Fig. 2. A newly fractured pyrite surface has an initial open-circuit potential near -0.4 V(SCE), which is consistent with the literature (5). Following fracture, the surface oxidizes with the potential increasing to the usual mixed potential value. In some experiments, it was desirable to prevent or minimize pyrite oxidization following fracture. For this purpose, the electrodes were potentiostated in the range -0.135 to -0.185 V(SHE) during fracture. The insert of Fig. 2 shows the current measured while potentiostating the pyrite electrode at -0.375 V during fracture. The current is anodic, establishing that a fresh pyrite surface oxidizes even at such a low potential. When the electrodes are potentiostated at -0.185 V during fracture, a cathodic current is observed, establishing that the fresh surface becomes slightly reduced. The exact potential at fracture is difficult to determine and may vary slightly from sample to sample, but it is very close to -0.16 V at pH 9.2. The amount of charge passed when holding the electrodes between -0.11 V and -0.185 V during fracture is less than a monolayer.

Fig. 3 shows a voltammetry curve on a fractured pyrite electrode. It is known that the anodic peak at -0.116 V represents the formation of ferric hydroxide and the cathodic peak at -0.31 V its reduction to ferrous-hydroxide (6). The ferric hydroxide is believed to form by reaction with elemental iron produced during the cathodic sweep.

On the positive sweep above 0.24 V, pyrite oxidizes by the reactions:

$$FeS_2 + 3H_2O = Fe(OH)_3 + 2S + 3H^+ + 3e, \text{ and} \quad (1)$$

$$FeS_2 + 11H_2O = Fe(OH)_3 + 2SO_4^{2-} + 19H^+ + 15e. \quad (2)$$

The amount of elemental sulfur produced by reaction 1 decreases, while the amount of sulfate by reaction 2 increases with increasing anodic potential (6). More recently, it has been suggested from XPS and electrochemical studies that the product of reaction 1 is not elemental sulfur but a metal polysulfide (7) or a metal deficient sulfide (8).

On electrodes held at -0.135 V during fracture and then subjected to a negative going sweep, the cathodic peak at -0.31 V is not observed, consistent with the assignment of this peak to the reduction of a ferric hydroxide formed during the prior positive sweep.

The increase in current on the negative going sweep below -0.56 V represents the reduction of pyrite by reactions of the form (6-9):

$$FeS_2 + H^+ + 2e = FeS + HS^-, \quad (3)$$

$$FeS_2 + xH^+ + 2e = FeS_{2-x} + xHS^-, \text{ and} \quad (4)$$

$$FeS_2 + 2H^+ + 4e = Fe + 2HS^-. \quad (5)$$

Figure 4 shows the photocurrent-potential curve obtained simultaneously with the cyclic

voltammetry curve of Figure 3. With the pyrite samples from this source, only anodic photocurrents are observed over the potential range of -0.76 to 0.64 V, indicating that the energy bands of pyrite are bent upwards. The maximum magnitude of the photocurrent on most samples was 10 to 15 percent of the current on the cyclic voltammetry curves. The photocurrent goes to zero when the electrodes are held for several minutes at -0.76 V, or during negative potential sweeps to about -0.96 V.

In general, the photocurrent indicates the band bending at the surface and the location of the redox potential of species in solution relative to the band edges of pyrite. The potential where a zero photocurrent is observed is often taken as the flat band potential, although trapping and recombination of photogenerated carriers in surface states may shift the zero photocurrent away from the flat band potential (V_{fb}). It can be assumed that the samples are highly n-type because of the lack of cathodic photocurrents at large negative potentials. The photocurrents therefore involve minority carriers (holes) from the valence band. The necessity to cathodically decompose pyrite at -0.76 V to reduce the photocurrent to zero establishes that the surface composition of pyrite must be altered (via reactions 3-5) to attain the flat band potential.

When potentiostating pyrite electrodes in the range of -0.11 to -0.185 V during fracture, a finite anodic photocurrent appears to be spontaneously present. It should be noted that at these potentials, pyrite does not oxidize to form $Fe(OH)_3$. With subsequent cyclic sweeps between -0.135 and -0.66 V, the photocurrent remains nearly constant, with the cathodic branch slightly larger than the anodic branch (Fig. 5). By preventing pyrite oxidation to $Fe(OH)_3$, most of the structure on the voltammetry curves and on the photocurrent curves during reduction is eliminated.

The well-defined peak in the photocurrent near -0.31 V on the negative going sweep (Fig. 4) occurs only after pyrite has been oxidized to form ferric hydroxide. A comparison of Figs. 3 and 4 indicates that the photocurrent peak is related to the voltammetry peak attributed to the reduction of ferric- to ferrous-hydroxide. This process occurs in the dark through charge exchange with the conduction band:

$$Fe(OH)_3 + e_{cb} = Fe(OH)_2 + OH^- \quad (6)$$

Holes generated in the valence band by the chopped illumination are believed to reoxidize Fe(II) by the reaction,

$$Fe(OH)_2 + OH^- + h_{vb} = Fe(OH)_3, \quad (7)$$

giving rise to the photocurrent peak during the negative sweep.

In addition, $FeOH^+$ or HS^- may be a reduction product during the negative going sweep that is produced by capture of a conduction band electron. The associated anodic photocurrent would then represent the re-oxidation of these species by capture of photogenerated holes from the valence band.

Several characteristics of the photocurrent behavior of pyrite suggest that an intrinsic surface state, possibly modified by hydroxide adsorption, dominates the interfacial behavior of pyrite. These characteristics are:

i) spontaneous anodic photocurrents on electrodes that are potentiostated, at fracture, under conditions where only slight oxidation or slight reduction occurs,

ii) weak dependence of the photocurrent on electrode potentials from -0.135 to -0.66 V, and

iii) the necessity to cathodically decompose pyrite to reach the flat band potential.

This behavior is consistent with an intrinsic surface state that produces a net negative charge on the surface and an underlying depletion layer (positive space charge layer on the n-type electrodes). The charge in the surface state is not readily neutralized; to the contrary, neutralization requires cathodic decomposition of the surface region of pyrite. Thus, the Fermi energy at the surface is pinned over a wide potential range ($\approx$-0.66 to 0.44 V), causing a quasi-metallic behavior where changes in electrode potential occur primarily across the Helmholtz layer.

The existence of an intrinsic surface state was suggested by Pettenkofer et al. (10) from photoemission studies on synthetic and natural pyrite. They observed three different sulfur states on the vacuum cleaved (100) surface of pyrite: two attributed to FeS_2 at the surface and in the bulk, and the third to an FeS-like surface state. They suggested that the FeS-like state represents a Tamm state arising from the reduced symmetry at the surface. From XPS measurements they reported that both the iron and sulfur 2p levels show chemical shifts from the S_2^{2-} in FeS_2 to S^{2-} in FeS, with Fe remaining nominally as Fe(II).

An intrinsic surface state is also consistent with studies of the photoelectrochemical behavior of pyrite with the redox couples V^{2+}/V^{3+}, Fe^{2+}/Fe^{3+}, Br^-/Br_2, and Cl^-/Cl_2. Jaegermann and Tributsch (11) and Salvador et al. (12) studied the anodic photocurrents for these redox couples and found that the results were consistent with the band edges shifting with the reversible

potential of the redox couples, implying that the flat band potential also shifts with the redox couple. They attributed the shifts to a high density of band gap states associated with Fe_2S_3 lattice impurities. Mishra and Osseo-Asare (13 15) observed similar shifts in the band edges of pyrite in acetonitrile with ferrocene and N,N,N',N'-tetramethyl-p-phenylenediamine redox couples. They also attributed the quasi-metallic behavior of pyrite, i.e., pinned surface Fermi energy and large dark currents, to surface states. Since Fermi level pinning was observed in the non-aqueous solution, they suggested that the surface states could not be attributed to hydrogen or hydroxyl ion adsorption.

In order to further investigate the relationship between the intrinsic surface state on pyrite and the composition of the surface, sulfur was deposited on an electrode by oxidizing HS^-. Fig. 6 shows a cyclic voltammetry curve in the presence of $3.3x10^{-3}$ M HS^-, and Fig. 7 the simultaneous photocurrent curve. The anodic peak near 0.04 V (Fig. 7) represents the oxidation of HS^- to S, and the cathodic peak at -0.61 the reverse process (16). At potentials between -0.76 and -0.16 V on the positive potential sweep, the photocurrent is similar to the behavior observed in the absence of hydrosulfide, i.e., zero photocurrent induced by cathodic dissolution of pyrite at -0.76 V and a gradual increase in photocurrent with increasing potential; however, sulfur deposition causes a sudden decrease in the photocurrent at potentials greater than -0.06 V. The decrease may be associated with either a decrease in band bending at the surface (i.e., an apparent shift in the flat band potential to more positive potentials, similar to the model proposed in references (11,12)), or to the formation of a passivating sulfur layer at the surface, which inhibits charge transfer. The decrease in current on the voltammetry curve with sulfur deposition indicates a passivated surface.

However, during the reduction cycle, there is a reduction process on the voltammetry curve commencing at -0.16 V which precedes the reduction of the sulfur deposited on the positive scan, possibly representing the reduction of an adsorbed sulfur species as a precursor to the reduction of elemental sulfur. In the absence of HS^-, $Fe(OH)_3$ is also reduced in this potential range, but its formation is not likely in the presence of HS^-. Interestingly, the photocurrent during the negative going scan rapidly increases before the dominant sulfur reduction process occurs. The overall behavior suggests that sulfur deposition neutralizes the charge in intrinsic surface states on pyrite, relaxing the upward bent bands and thereby decreasing the photocurrent. With sufficient neutralization of the charge in surface states, an apparent positive shift of about 1 V occurs in the flat band potential. This is the same behavior observed by others for several different redox couples (11-15). It should be noted that the photocurrent does not go entirely to zero with sulfur deposition; thus, the actual flat band potential is not determined. A shift to more positive values is inferred from the decrease in photocurrent.

Polysulfides (7), a metal deficient layer surface layer (8), and elemental sulfur (17) have all been postulated as oxidation products that produce excess sulfur on pyrite. The neutralization of the charge in the intrinsic surface state by the oxidation of pyrite to produce excess sulfur at the surface may offer an explanation for the apparent shifts in the band edges of pyrite with the potential of various redox couples.

Finally, it should be noted that polishing a fractured surface with 600 grit abrasive reduces the photocurrent on pyrite by a factor of 10 to 50, at equivalent light intensities. Because the photocurrents after polishing were reduced to approximately the noise level of our measuring system, no attempt was made to further quantify how polishing affects the reactivity of the

electrodes for charge transfer processes; however, polishing produces defect states at the surface and deep beneath the surface. These states obviously act as recombination centers, reducing the lifetime of photogenerated holes and hence the photoresponse, and also act as trapping centers, providing additional charge storage capacity at and beneath the surface which causes further pinning (above that of intrinsic surface states, for example) of the Fermi level at the surface. Fermi level pinning, shortened carrier lifetimes, and new surface energy levels caused by polishing defects could conceivably alter charge transfer reactions at pyrite surfaces. Most research in sulfide electrochemistry related to flotation utilizes polished electrodes. Fractured surfaces are probably more similar to the surfaces produced by comminution; therefore, the effect of polishing on adsorption and charge transfer processes at sulfide surfaces is an area that should receive some attention. Controlling the flotation of sulfide minerals often involves the adsorption of relatively small quantities of surfactants. It is the submonolayer quantities that would likely be sensitive to surface defects.

CONCLUSIONS

Transient photocurrent measurements show that a depletion layer forms spontaneously on freshly fractured pyrite surfaces, in contrast to galena, which assumes the flat band potential at cleavage and a depletion layer by subsequent oxidation (18). The characteristics of the photocurrent as a function of electrode potential indicate that the depletion layer arises from an excess of negative charge associated with an intrinsic, acceptor-like surface state on the fractured surface. To obtain a flat band potential on pyrite, the electrode has to be cathodically decomposed at potentials where sulfur is removed from the surface. Alternatively, the

deposition of sulfur on pyrite surfaces from a hydrosulfide solution causes an apparent 1 V shift in the flat band potential, which may not represent a true shift in the flat band potential but rather a partial neutralization of the charge in the intrinsic surface state that causes a large decrease in band bending.

The existence of a surface state on pyrite surfaces can logically be assumed to be important in the flotation of pyrite because the surface states control how a change in interfacial potential is distributed between the Helmholtz layer and the space charge layer of pyrite. The distribution of this potential can be expected to regulate the energetics and kinetics of pyrite oxidation as well as the adsorption of reagents used in flotation.

It is also shown that polishing introduces defect centers at the surface and in the space charge region of pyrite, greatly reducing the photoresponse of the electrodes and may also have unknown effects on the electrochemical reactivity of pyrite.

REFERENCES

1. Heyes, G.W. and Trahar, W.J., "The natural floatability of chalcopyrite," Int. J. Miner. Process, 4:317-344, 1977.

2. Luttrell, G.H. and Yoon, R.-H., "Surface studies of the collectorless flotation of chalcopyrite," Colloids Surf., 12:239-254, 1984.

3. Lai, R.W., Diehl, J.R., Hammack, R.W. and Khan, U.M., "Comparative study of the surface properties and the reactivity of coal pyrite and mineral pyrite," Trans. Miner. and Metall. Proc. 7:1, 43-48, 1990.

4. Richardson, P.E., Li. Y, and Yoon, R.-H, "The photoelectrochemistry of *in situ* fractured pyrite electrodes," To be published as an extended abstract for the Electrochemical Society Annual Meeting, May 17-22, 1991.

5. T. Chmielewski, and T.D. Wheelock, J. Mining & Metallurgy, **26**(2), pp. 133-144 (1990).

6. I.C. Hamilton and R. Woods, J. Electroanal. Chem., **118**, pp. 327-343 (1981).

7. Yoon, R.-H., Lagno, M.L., Luttrell, G.H., and Mielczarski, J. A., On the Hydrophobicity of coal pyrite after electrochemical alteration. Processing and Utilization of High Sulfur Coals IV, Ed. by P.R. Dugan, D.R. Quigley, and Y.A. Attia. Elsevier Science Pubs., Amsterdam, 1991.

8. A.N. Buckley and R. Woods, Applied Surface Sci. **27**, (1987) 437-452.

9. Shu, X, Wadsworth, M.E., Bodily, D.M. and Riley, A.M., "Surface properties of mineral and coal pyrite after electrochemical alteration," Processing and Utilization of High Sulfur Coals IV, ed. P.R. Dugan, D.R. Quigley and Y.A. Attia, Elsevier Sci. Pub B.V. Amsterdam, 1991.

10. C. Pettenkofer, W. Jaegermann, H. Tributsch, H.Kuhlenbeck, W.Braun, and S. Bernstorff, in 5th Proceedings, Latin American Symp. on Surf. Physics, CIF Series, **II**, edited by M. Cardona and J. Giraldo, pp. 243-255 (1988).

11. W. Jaegermann, and H. Tributsch, J. Appl. Electrochem.,**13**, 743 (1983).

12. P. Salvador and D.Tafalla, J. Electrochem. Soc., **11**, Vol. 138, pp. 3361-3369 (1991).

13. K.K. Mishra and K. Osseo-Asare, J. Electrochem. Soc. **135**, pp. 1898-1901 (1988).

14. K.K. Mishra and K. Osseo-Asare, J. Electrochem, Soc. 135, pp. 2502-2509 (1988).

15. K.K. Mishra and K. Osseo-Asare, J. Electrochem. Soc.**139**, No. 3, pp. 749-752 (1992).

16. Walker, G.W., Walters, C.P. and Richardson, P.E., "Hydrophobic effects of sulfur and xanthate on metal and mineral electrodes," Int. J. Miner. Process., **18**:119-137, 1986.

17. Kleinmann, R.P.A., Crerar, D.A. and Pacelli, R.R., "Biogeochemistry of acid mine drainage and a method to control formation," Mining Engineering, Mar. 1981.

18. Richardson, P.E. and O'Dell, C.S., "Semiconducting Characteristics of Galena Electrodes," J. Electrochem. Soc. **132** (6), pp. 1350-1356, 1985.

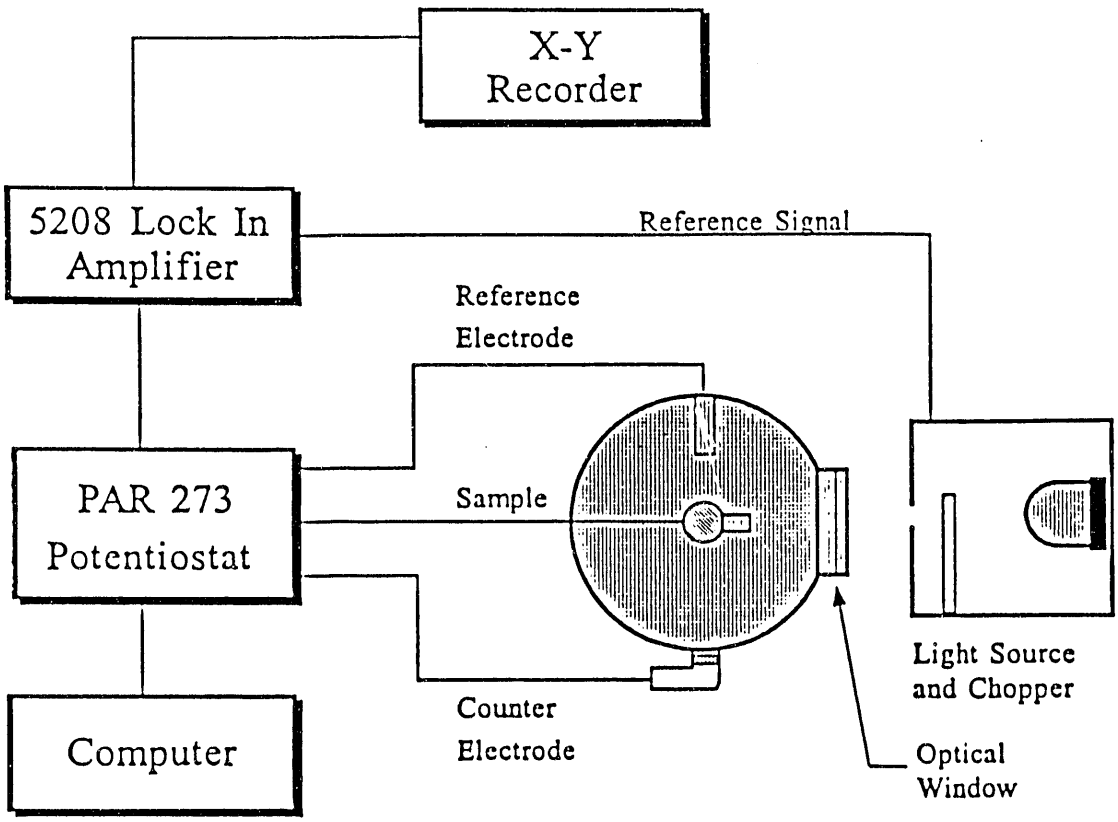

Fig.1. Schematic of experimental set-up for photocurrent measurements.

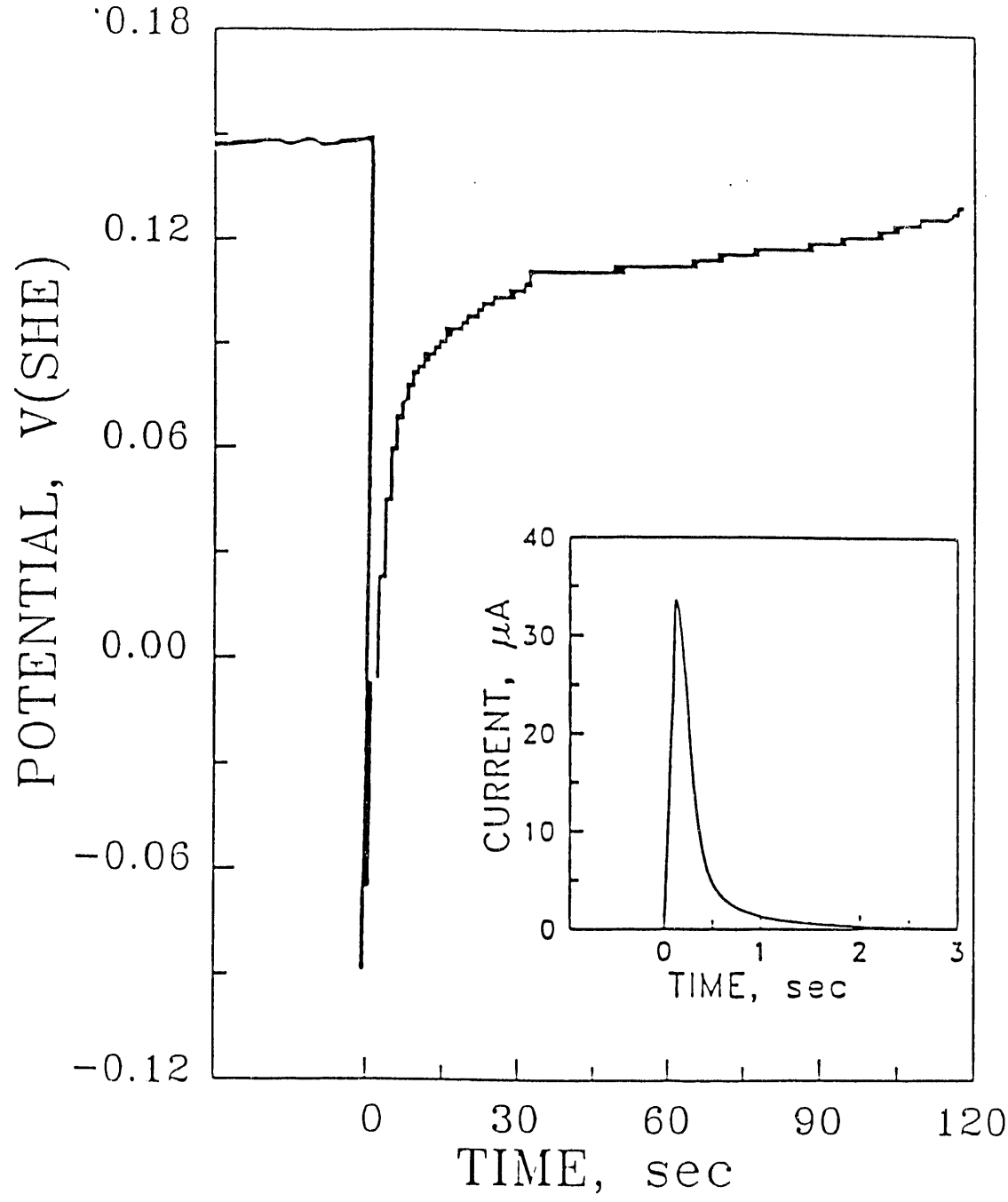

Fig.2. Open-circuit potential vs. time for a freshly fractured pyrite electrode. Insert, anodic current passed when fracturing a pyrite electrode held at -0.134 V(SHE).

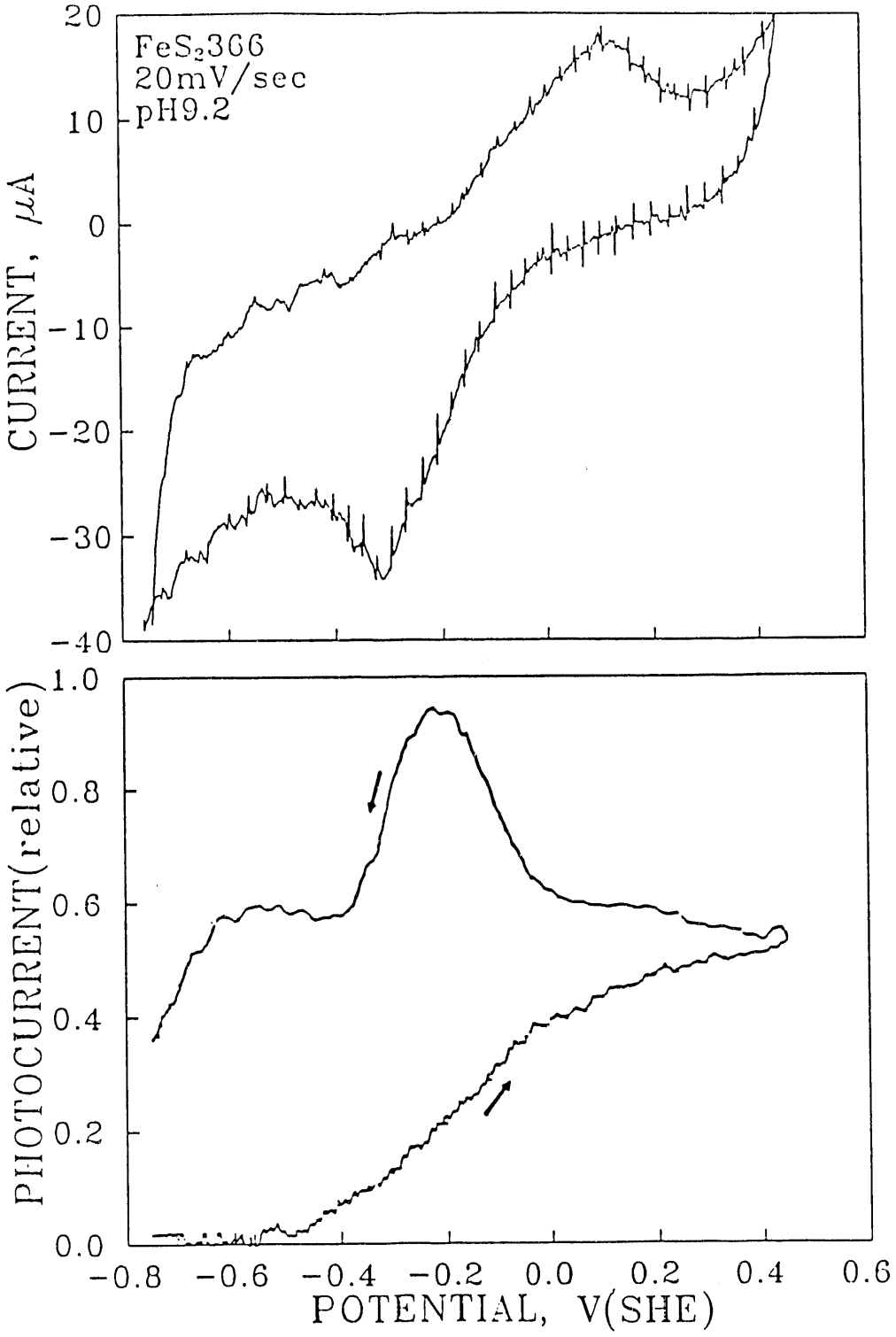

Fig.3. (top) Voltammetry of freshly fractured pyrite electrode.

Fig.4. (bottom) Photocurrent of a fractured pyrite electrode obtained simultaneously with voltammetry curve of Fig.3.

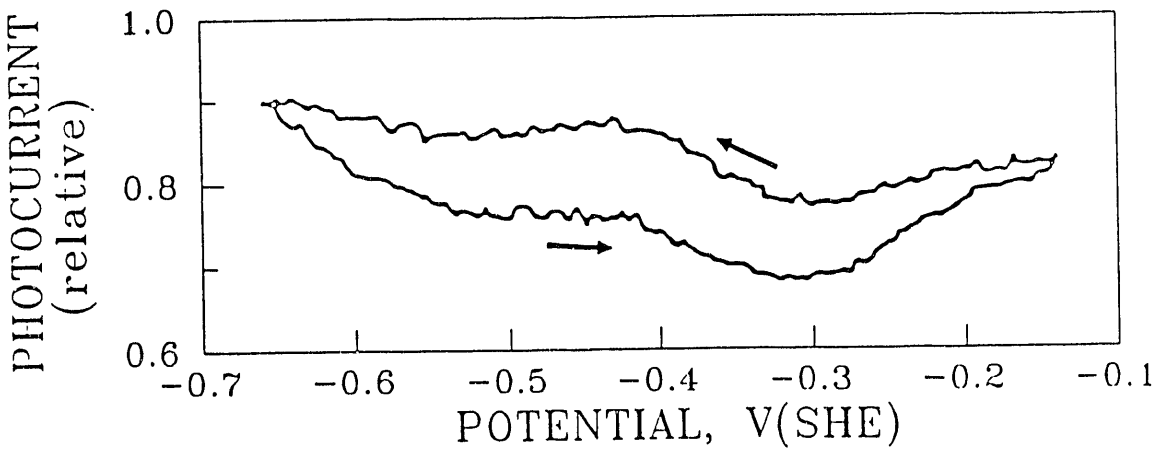

Fig.5. Photocurrent of pyrite electrode during the first negative and subsequent positive potential sweeps after fracture. Electrode held at -0.134 V(SHE) during fracture. Sweep rate is 5 mV/sec.

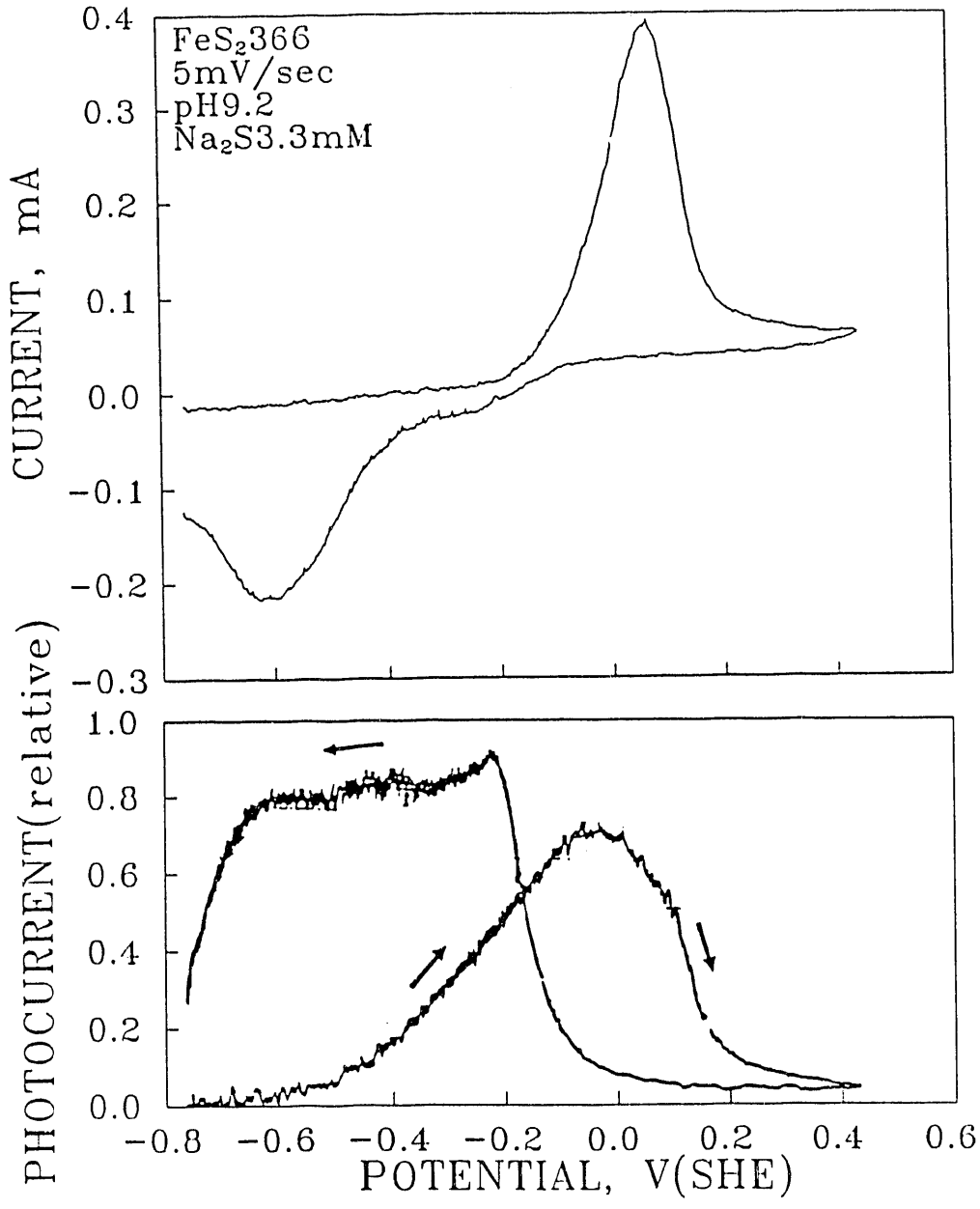

Fig.6. (top) Voltammetry of a fractured pyrite electrode in 3.3 mM Na_2S. Sweep rate is 5 mV/sec.

Fig.7. (bottom) Photocurrent of a fractured pyrite electrode in 3.3 mM Na_2S. Curve obtained simultaneously with the voltammetry curve of Fig.6.

END

DATE
FILMED
4 / 14 / 93